2022

Assessment Of The Accuracy Of Solar Irradiance Models In Mountain Locations: The Case Of Bolzano, Italy

Giovanni Pernigotto

Alessandro Prada

Andrea Gasparella

Assessment Of The Accuracy Of Solar Irradiance Models In Mountain Locations: The Case Of Bolzano, Italy

Giovanni PERNIGOTTO[1]*, Alessandro PRADA[2], Andrea GASPARELLA[3]

[1]Free University of Bozen-Bolzano, Faculty of Science and Technology,
Bolzano, Italy
Tel: +39 0471 017632, Fax: +39 0471 017009, email: giovanni.pernigotto@unibz.it

[2]University of Trento, Department of Civil Environmental and Mechanical Engineering,
Trento, Italy
Tel: +39 0461 282516, Fax: +39 0461 282672, email: alessandro.prada@unitn.it

[3]Free University of Bozen-Bolzano, Faculty of Science and Technology,
Bolzano, Italy
Tel: +39 0471 017200, Fax: +39 0471 017009, email: andrea.gasparella@unibz.it

* Corresponding Author

ABSTRACT

Two main groups of solar irradiance models can be identified in the literature: the "*horizontal diffuse irradiance models*", whose goal is to process the global horizontal irradiance to calculate the beam and the diffuse components, and the "*irradiance models for tilted surfaces*", which are used to determine the solar radiation incident on generic surfaces starting from the horizontal measured data, if beam and diffuse components are available, or from the results of a model of the first group. According to the state-of-the-art, there is no pair of "*horizontal diffuse irradiance model*" and "*irradiance model for tilted surfaces*" which can give the same level of accuracy worldwide, since they were developed starting from solar irradiance data of specific meteorological stations, with typical weather and sky cover conditions. In addition, this becomes particularly critical for locations in mountain regions, characterized by many natural obstacles altering the view of the sky, its radiance distributions, as well as the ground reflections in a very dynamic and localized way, with an impact on the solar diffuse and beam radiation available.
In this research, the performance of 22 "*horizontal diffuse irradiance models*" and 12 "*irradiance models for tilted surfaces*" were discussed, using as benchmark the global solar irradiance data collected for both horizontal and vertical surfaces in a multi-year solar monitoring campaign performed in Bolzano, a city in the Italian Alps. After identifying the most and the least accurate models, they were adopted to simulate the energy needs for space heating and cooling for a dataset of 48 simplified building configurations, in order to discuss the impact of the calculated incident solar irradiance on the simulated building energy performance.

1. INTRODUCTION

In order to minimize its energy demand, a high performance building has to carefully manage the solar radiation received on its external envelope, especially on the transparent elements. Indeed, solar gains are crucial to reduce the space heating load during the cold season, even if proper controls are required to avoid overheating and cooling peak loads during the hot one. As a whole, an optimal control of solar gains can ensure the achievement of higher energy performance, preserving or increasing thermal and visual comfort. Nevertheless, extensive application of advanced solar controls can be technically challenging or too expensive to adopt, making still very common solutions based on the assessment of vertical solar irradiance on the main façade or of horizontal irradiance on the roof. In both

cases, the measured irradiance is the global one, without distinguishing between beam and diffuse components, albeit their different impact on the performance and on specific control algorithms. In these contexts, solar irradiance models can be used to increase the information detail.
Several empirical models were proposed in the literature, to distinguish the horizontal solar irradiation into beam and diffuse components (*horizontal diffuse irradiance models*) and to calculate the irradiation on tilted surfaces (*irradiance models for tilted surfaces*). Nevertheless, their empirical nature means that the model accuracy is closely tied to site characteristics, since every model was developed minimizing the deviation to experimental data collected in specific locations. For this reason, constant and accurate reliability cannot be taken for granted by changing location and climate.
In (Dervishi and Mahdavi, 2012), the authors assessed the model accuracy by comparing the models' predictions against experimental data, drawing some conclusions about the best model for a given locality. Other researches (Prada *et al.*, 2014a, 2014b, 2015; Pernigotto *et al.*, 2015 and 2016), instead, quantified the effect of the different models on the Building Energy Simulation *BES* prediction by highlighting the building characteristics increasing the sensitivity of *BES* to the selection of solar irradiance models. This is, for instance, a problematic issue when irradiance models, mostly derived in flat regions, are used to evaluate the micro-climatic boundary conditions in mountain contexts, where the complex irradiation patterns depend on the orography and the multiple terrain reflections.
Further expanding previous analyses, in this work we investigated the effect of the choice of solar irradiation models on the uncertainty of the predicted energy performance in the Alpine city of Bolzano, Italy. 22 *horizontal diffuse irradiance models* were coupled with 12 *irradiance models for tilted surfaces* and tested against the experimental data collected in Bolzano. A subset of models with extreme behavior were selected from the statistical comparison between model predictions and measurements on vertical surfaces oriented towards the main cardinal points. The different solar radiation patterns were then used as input in TRNSYS 18 for the simulation of the energy performances of a dataset of 48 simplified residential buildings, built varying parametrically insulation and thermal inertia of opaque components, windows surface and orientation, and solar heat gain coefficient of glazing.

2. METHODS

This section describes the methods adopted for the development of this research. After the description of the case-study mountain location of Bolzano, Italy, as well as the features of the considered weather station, the list of the selected solar irradiance models is presented. Finally, the dataset of building models simulated with TRNSYS 18 to assess the accuracy of a subset of solar irradiance models is illustrated.

2.1 Case-study location and weather station

Bolzano is an Italian municipality in the middle of the Alps (46.500° N, 11.350° E), specifically in a basin where three valleys - Sarntal, Eisacktal, and the Adige Valley, and their rivers, respectively, Talfer-Talvera, Eisack-Isarco, and Adige, meet. The settlement area occupies a surface of about 30 km^2, where almost 110'000 people live. The municipality spreads from 232 m to more than 1600 m above the sea level; however, the city center is located at an altitude of 262 m.
The weather station considered in this study was designed by the Research Group in Building Physics of the Free University of Bozen-Bolzano and installed in 2017 on the flat green roof of one of the buildings of the university campus in the city center, specifically the Building E (46.498° N, 11.349° E), characterized by a height of about 25 m. Figure 1 shows a map of the basin of Bolzano with the university campus in the city center (red dot in the figure).
The urban layout of the city center of Bolzano is pretty homogeneous, with buildings surrounding the university campus with similar or lower heights compared to the Building E. Consequently, the main obstacles reducing the solar irradiance received on the roof where the weather station is installed are the natural ones, i.e., the mountains around the basin of Bolzano (Figure 2). In detail, it can be observed that the obstacles south of the weather station are small (with an altitude generally lower than 5°) while those found on the north-east and north-west are more significant. In particular, the obstacles' maximum altitude (about 30°) can be located on the north-west direction.
As regards the weather station, it is equipped with 5 EKO MS-802 pyranometers, respectively one installed horizontally for the measurement of the global horizontal irradiance and four installed vertically towards the main cardinal directions for the collection of the global irradiance incident on those orientations. Furthermore, the weather

station includes a EKO MS-56 pyrheliometer and a EKO MS-802 pyranometer, fixed on a STR-22G EKO sun-tracker station, for the measurement of the direct normal irradiance *DNI* and the diffuse component of the horizontal irradiance. Despite the availability of *DNI* and diffuse horizontal irradiance, the study presented in this paper considered only the global irradiance values recorded by the MS-802 pyranometers, representing data more commonly found in other weather stations in this mountain region, facilitating comparisons in the next developments of this research.

As mentioned above, the weather station was installed in 2017 and has collected solar data with 1-minute time-discretization since then. In the current research, data referred to years 2018, 2019 and 2021 were included. The year 2020 was not considered since the pandemic lockdowns prevented periodical maintenance of pyranometers.

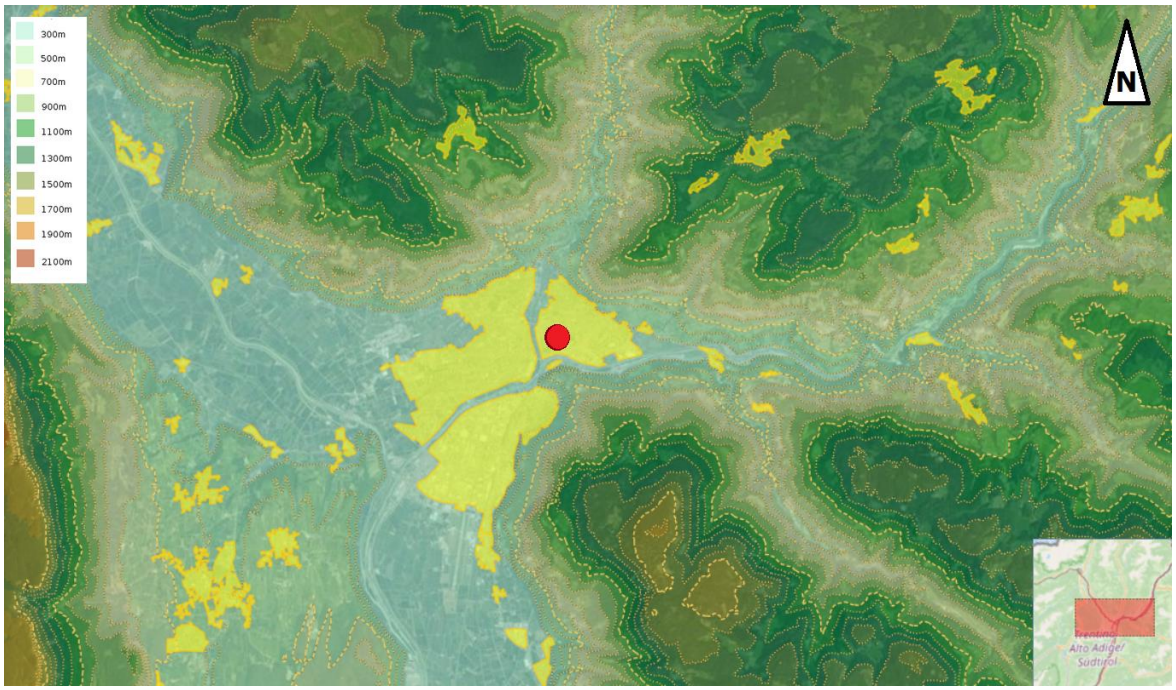

Figure 1: Basin of Bolzano: the different colors (light green to brown) identify the altitude while the yellow the urban areas; the red dot indicates the position of the university campus. Map developed from the Geobrowser Maps by the Autonomous Province of Bolzano

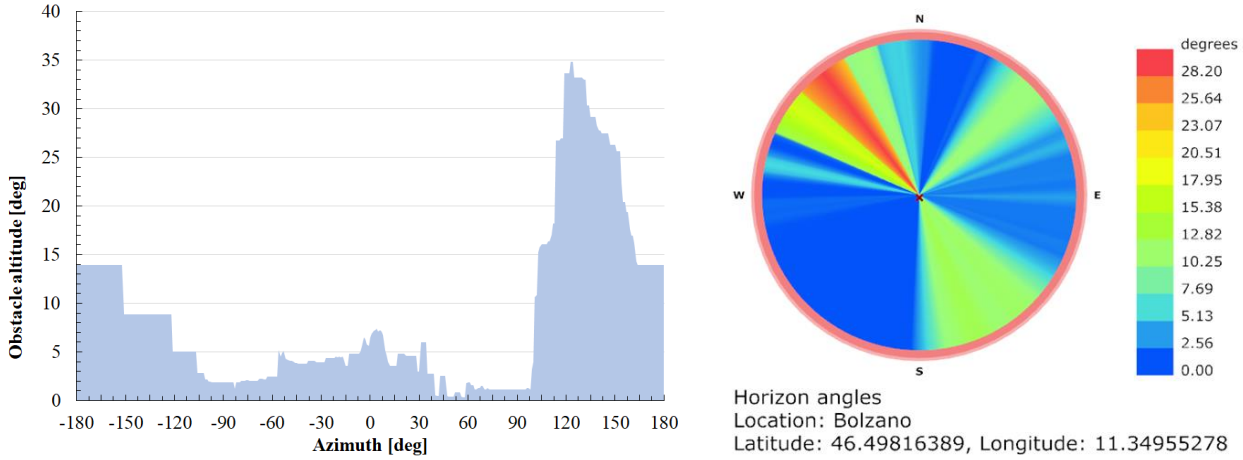

Figure 2: Altitude and position of the natural obstacles as determined with Grass GIS considering the Digital Surface Model *DSM* 2.5 m and the Digital Terrain Model *DTM* 2.5 m by the Autonomous Province of Bolzano

2.2 Solar irradiance models

As a follow-up to previous researches on this topic (Prada *et al.*, 2014a and 2014b; Pernigotto *et al.*, 2015 and 2016), we considered the same 22 *horizontal diffuse irradiance models* and 12 *irradiance models for tilted surfaces* analyzed before and reported in Table 1. In agreement with the approach in (Pernigotto *et al.*, 2016), the two groups of irradiance models were combined, for a total of 264 alternatives.

Table 1: Solar irradiance models

ID	*Horizontal diffuse irradiance models*	ID	*Irradiance models for tilted surfaces*
1	Erbs *et al.* (1982)	A	Liu & Jordan (1960)
2	Orgill & Hollands (1977)	B	Burgler (1977)
3	Reindl *et al.* (1990a) – Model 1	C	Temps & Coulson (1977)
4	Reindl *et al.* (1990a) – Model 2	D	Klucher (1978)
5	Reindl *et al.* (1990a) – Model 3	E	Hay & Davies (1980)
6	Lam & Li (1996)	F	Ma & Iqbal (1983)
7	Boland *et al.* (2008)	G	Skartveit & Olseth (1986)
8	Hawlader (1984)	H	Gueymard (1986)
9	De Miguel *et al.* (2001)	I	Reindl *et al.* (1990b)
10	Karatasou *et al.* (2003)	J	Perez *et al.* (1990)
11	Chandrasekaran & Kumar (1994)	K	Muneer (2006) – Model 1
12	Oliveira *et al.* (2002)	L	Muneer (2006) – Model 2
13	Soares *et al.* (2004)		
14	Muneer *et al.* (1984)		
15	Spencer (1982)		
16	Chendo & Maduekwe (1994) – Model 1		
17	Chendo & Maduekwe (1994) – Model 2		
18	Skartveit & Olseth (1987)		
19	Maxwell (1987)		
20	Perez *et al.* (1992) – Model 1		
21	Perez *et al.* (1992) – Model 2		
22	Perez *et al.* (1992) – Model 3		

2.3 Dataset of building configurations

A dataset of 48 simplified buildings was employed to assess the impact of the solar irradiance models on the simulated energy needs for space heating and cooling. All 48 building configurations have the same geometry, i.e., a thermal zone with a square floor area of 100 m^2, an internal height of 3 m, and the façades oriented towards the main cardinal directions. For each case, all windows are positioned on the same façade. Both sides of the vertical walls and the internal side of the roof have a solar absorptance of 0.3 while the external side of the roof and the internal side of the floor have 0.6.

All opaque components have the same composition, i.e., a two-layer structure with insulation on the external side and a massive layer whose thermal resistance is around 0.8 m^2 K W^{-1}. The insulating layer is polystyrene (thermal conductivity: 0.04 W m^{-1} K^{-1}; density: 40 kg m^{-3}; specific heat capacity: 1470 J kg^{-1} K^{-1}) while the massive layer can be either timber (thickness: 0.10 m; thermal conductivity: 0.13 W m^{-1} K^{-1}; density: 399 kg m^{-3}; specific heat capacity: 1880 J kg^{-1} K^{-1}) or concrete (thickness: 0.30 m; thermal conductivity: 0.37 W m^{-1} K^{-1}; density: 1190 kg m^{-3}; specific heat capacity: 840 J kg^{-1} K^{-1}). Windows are composed by a double-pane glazing with a *U*-value of 1.1 W m^{-2} K^{-1} and a timber frame (20 % of the window's area) with a *U*-value of 1.2 W m^{-2} K^{-1}.

Internal gains and ventilation rate are assumed constant and equal, respectively, to 4 W m^{-2}, half radiative and half convective, and to 0.3 air changes per hour, as indicated by the Italian technical specification UNI/TS 11300-1:2014 (UNI, 2014) for residential buildings. An ideal system provides all the power needed to maintain the zone internal air temperature between the heating and the cooling setpoints of 20 °C and 26 °C. Although for the climate of Bolzano the heating season starts on October 15th and finishes on April 15th, we assumed space heating and cooling

available all year, whenever needed. Further details about the dataset of buildings can be found in (Pernigotto *et al.*, 2021). Table 2 reports an overview of the variables differentiating the buildings in the dataset.

Table 2: Variables differentiating the buildings in the dataset

Insulation thickness and *U*-value	**Materials and thermal inertia *c***	**Windows' *SHGC***	**Windows' size and window-to-wall ratio *WWR***	**Windows orientation**
5 cm (U = 0.45 W m^{-2} K^{-1})	Timber (c = 75 kJ m^{-2} K^{-1})	*SHGC* = 0.35	14.56 m^2 (*WWR* = 48.5 %)	East
15 cm (U = 0.21 W m^{-2} K^{-1})	Concrete (c = 300 kJ m^{-2} K^{-1})	*SHGC* = 0.61	29.12 m^2 (*WWR* = 97.1 %)	South
-	-	-	-	West

2.4 Analysis methodology

The first step of the analysis regarded the data collected by the pyranometers of the weather station on top of the Building E of the university campus. A quality check was performed, in order to identify outliers and missing entries. For instance, values exceeding the solar constant and positive values before dawn and after dusk were removed. Input data, with 1-minute time discretization, were processed in order to get hourly profiles of solar irradiation expressed in watthours per square meter, as they are conventionally found in weather data for building performance simulation (see, for instance, the EnergyPlus .epw weather files). Minor missing entries (i.e., one or few hours of missing solar irradiation data) were fixed by linear or cyclic interpolation, depending on the case. On the contrary, larger missing data entries, longer than a day, were not fixed and simply not involved in the analysis.

The second step was dedicated to the assessment of the irradiance models against the measured solar data. The hourly profiles of global solar horizontal irradiation of 2018, 2019 and 2021 were used as inputs to calculate the global solar irradiation on four vertical surfaces oriented towards the main cardinal directions, using each one of the 264 combinations of pairs of *horizontal diffuse irradiance models* and *irradiance models for tilted surfaces*. The determined hourly profiles of global solar irradiation on vertical surfaces were compared to the measured ones, calculating for each orientation the Mean Absolute Error *MAE*. This index was exploited to identify the best- and the worst-performing pairs of irradiance models, as well as those *horizontal diffuse irradiance models* and *irradiance models for tilted surfaces* most frequently found among the best- and the worst-performing ones (i.e., those with the minimum and the maximum values of *MAE*).

The last step considered those *horizontal diffuse irradiance models* and *irradiance models for tilted surfaces* most frequently found among the best- and the worst-performing ones. Those models were used to determine the solar irradiance incident on the external envelope of the dataset of 48 buildings, respectively for 2018, 2019 and 2021, and simulate with TRNSYS 18 their energy needs for space heating and cooling. The goal of this final assessment was to discuss the variability which can be found in building performance simulation because of the selection of solar irradiance models when applied in mountain environments, as well as those building configurations more affected by the choice of solar irradiance models for the specific location of Bolzano.

3. RESULTS AND DISCUSSION

3.1 Dataset of solar irradiation measurements

The quality check for the three available years allowed us to identify those series of hourly data of solar irradiation with missing or wrong entries, as reported in Table 3. As it can be noticed, although the year 2021 is characterized by a larger share of missing data, its numerosity can be still considered adequate for a robust comparison. As specified in Section 2.4, these series were discarded in the rest of the analysis and, as regards the last step, the corresponding months (February 2018, August 2019, April and May 2021) not even simulated.

3.2 Comparison between simulated and measured solar irradiation values

The Mean Absolute Error was used as index to identify, for each year and for the whole series, which pairs of solar irradiance models gave the closest estimates to the actual recordings for the four vertical cardinal directions.

Table 3: Quality check on the solar irradiation measurements

Year	Sunshine hours for vertical surfaces [h]				Missing data [h]	Period missing
	South	East	North	West		
2018	4641	4652	4654	4657	83	8 days in February
2019	4661	4661	4660	4660	81	5 days in August and 1 day in September
2021	4217	4212	4216	4218	522	34 days in April and May

Table 4: Best- and worst-performing pairs of solar irradiance models and respective *MAE* (Wh m^{-2}) for the three considered years and the four cardinal orientations. In grey those pairs confirmed in multiple years. See Table 1 for the model identification

	Best-performing pairs of irradiance models				Worst-performing pairs of irradiance models			
	South	East	North	West	South	East	North	West
2018	A5 41.7	C20 78.6	J18 22.7	B20 163.5	C20 59.6	F15 134.5	D20 76.9	F5 335.0
2019	H18 44.1	C18 70.7	J13 31.7	B20 160.7	F15 75.3	I15 111.6	J20 129.4	J20 469.2
2021	H18 45.7	C20 81.5	J18 22.9	B20 172.5	F18 69.1	F15 147.6	D20 77.8	F18 377.5
Similarity among the years	**67 %**	**83 %**	**83 %**	**100 %**	**33 %**	**83 %**	**83 %**	**33 %**
ALL	H18 43.8	C20 79.3	J18 26.1	B20 165.3	I15 67.4	F15 130.6	D20 79.9	F18 384.1

As it can be noticed in Table 4, the *MAEs* assessed over the three years combined vary significantly changing orientation and comparing best- and worst-performing pairs of solar irradiance models. The south orientation is well-predicted, with an average *MAE* around 40-45 Wh m^{-2} for the best-performing pairs and around 60-75 Wh m^{-2} for the worst-performing ones. Although the same index for the north-orientation is smaller, its relative incidence is high, considering that this orientation receives predominantly diffuse irradiance. Moreover, the worst-performing pairs of models show *MAEs* which are more than three times those of the best-performing models. East and west-orientation are characterized by larger errors in the irradiation estimation. Specifically, the *MAEs* for east-oriented walls range from about 80 Wh m^{-2} (best-performing pairs of models) to 110-150 Wh m^{-2} (worst-performing ones). Finally, the west-orientation is the most critical one, with Mean Absolute Errors larger than 160 Wh m^{-2} for the best-performing models and in the range 330-470 Wh m^{-2} for the worst-performing ones. This is somehow expected: indeed, as observed in Section 2.1, north-east and north-west show the presence of the most important obstacles
The best- and the worst-performing models are found different for each orientation and, considering that the different years have various missing entries, not always constant along the time-series. Nevertheless, some trends can be identified. Gueymard + Skartveit & Olseth (**H18**), Temps & Coulson + Perez *et al.* Model 1 (**C20**), Perez *et al.* + Skartveit & Olseth (**J18**) and Burgler + Perez *et al.* Model 1 (**B20**) are the best solutions, respectively for the south-, east-, north- and west-orientation. On the contrary, Ma & Iqbal + Spencer (**F15**) and Klucher + Perez *et al.* Model 1 (**D20**) show the worst performance for east- and north-orientations.

Table 5 and Table 6 show, respectively, the *horizontal diffuse irradiance models* and *irradiance models for tilted surfaces* most frequently found among the best- and the worst-performing ones.
For east- and west-oriented vertical components, the Perez *et al.* Model 1 (**20**) is often the most accurate *horizontal diffuse irradiance model* while the very same model happens to be the worst-performing one, when it comes to the

north-oriented vertical elements. As a whole, the Spencer model (**15**) is generally the worst-performing *horizontal diffuse irradiance model* for the remaining orientations.
The best-performing *irradiance model for tilted surfaces* depends on the considered vertical orientation: the Burgler model (**B**) is the best-performing one for south- and west-oriented elements, the model by Temps & Coulson (**C**) is more accurate for the east-facing ones, while the Perez model (**J**) is superior for the north orientation. As regards the worst-performing *irradiance model for tilted surfaces*, the model by Ma & Iqbal (**F**) is the worst-performing one for all orientations but the north, for which the model by Klucher (**D**) is more frequently the one leading to the largest errors.

In consideration of the results found in this section, the following list of irradiance models was considered for the last step of the analysis involving building performance simulation:

- *horizontal diffuse irradiance models*: the Spencer model (**15**) and the Perez *et al.* Model 1 (**20**);
- *irradiance model for tilted surfaces*: the Burgler model (**B**), the model by Temps & Coulson (**C**), the model by Klucher (**D**), the model by Ma & Iqbal (**F**), and the Perez model (**J**).

Table 5: Best- and worst-performing *horizontal diffuse irradiance models* for the three considered years and the four cardinal orientations. In grey those models confirmed in multiple years. See Table 1 for the model identification

	Best-performing horizontal diffuse irradiance models				**Worst-performing horizontal diffuse irradiance models**			
	South	**East**	**North**	**West**	**South**	**East**	**North**	**West**
2018	18	20	13	20	15	15	20	15
2019	5	20	15	20	15	15	20	5
2021	18	20	18	20	15	15	20	15
Similarity among the years	**67 %**	**100 %**	**0 %**	**100 %**	**100 %**	**100 %**	**100 %**	**67 %**
ALL	5	20	6 / 13	20	15	15	20	5 / 15

Table 6: Best- and worst-performing *irradiance models for tilted surfaces* for the three considered years and the four cardinal orientations. In grey those models confirmed in multiple years. See Table 1 for the model identification

	Best-performing irradiance models for tilted surfaces				**Worst-performing irradiance models for tilted surfaces**			
	South	**East**	**North**	**West**	**South**	**East**	**North**	**West**
2018	B	C	J	B	F	F	D	F
2019	K	C	J	B	F	F	D	F
2021	B	C	J	B	F	F	D	F
Similarity among the years	**67 %**	**100 %**	**100 %**	**100 %**	**100 %**	**100 %**	**100 %**	**100 %**
ALL	B	C	J	B	F	F	D	F

3.3 Analysis of building energy needs

TRNSYS simulations were run for each of the 48 building configurations and the three considered years. As mentioned in Section 2.4, the months with long series of missing data reported in Table 3 were discarded: simulation start was fixed at the next month after those series (i.e., March, September and June, respectively for 2018, 2019 and 2021) and simulation stop before them (i.e., January, July and March, respectively for 2018, 2019 and 2021). Energy

needs for space heating and cooling were analyzed at both monthly and annual basis. Table 7 reports the minimum and the maximum deviations found simulating the dataset of buildings with the 10 different pairs of solar irradiance models selected in Section 3.2.

Table 7: Minimum and maximum monthly and annual deviations of heating and cooling needs for the simulated dataset of 48 buildings. The grey cells indicate the non-simulated months while the crossed ones represent those months without energy demand

	Heating need deviations [kWh m^{-2}]						**Cooling need deviations [kWh m^{-2}]**					
	2018		**2019**		**2021**		**2018**		**2019**		**2021**	
	min	**max**	**min**	**max**	**min**	**max**	**min**	**max**	**min**	**max**	**min**	**max**
Jan	0.4	4.1	0.5	5.2	0.5	5.3	0.0	1.2	0.0	1.7		
Feb			0.9	4.0	0.8	3.6			0.0	4.6	0.0	3.6
Mar	0.7	2.4	0.0	2.8	0.0	3.8	0.0	3.9	0.0	9.6	0.0	9.6
Apr	0.0	1.1	0.0	1.4			0.0	7.0	0.0	5.6		
May			0.0	1.5			0.0	6.7	0.0	10.2		
Jun							1.5	7.2	2.4	44.9	1.4	6.4
Jul							1.6	7.7	2.1	33.7	1.4	7.7
Aug							1.1	9.6			0.9	9.4
Sep							0.3	8.7	0.0	6.2	0.3	9.2
Oct	0.0	1.0	0.0	1.4	0.0	2.2	0.0	5.9	0.0	4.5	0.0	5.3
Nov	0.4	3.3	0.3	2.6	0.6	4.4	0.0	1.1			0.0	2.4
Dec	0.4	4.9	0.3	4.2	0.4	4.9						
Period	**2.8**	**14.3**	**4.7**	**16.2**	**4.4**	**19.6**	**5.0**	**51.9**	**4.7**	**100.7**	**4.2**	**47.9**

As far as the heating needs are concerned, the largest deviations are usually found in the coldest months of the year and are around 5 kWh m^{-2} m^{-1}. Considering the whole simulated period, the largest deviations can range from 14 to 20 kWh m^{-2} a^{-1}. However, they are not related to the configurations with the largest energy needs for space heating but to the one with only 5-cm insulation on a concrete structure and large south-oriented windows with high *SHGC*. Analyzing the configurations with annual heating deviations larger than 10 kWh m^{-2} a^{-1}, it can be noticed that buildings with large south-oriented windows with high *SHGC* and poorly insulated concrete structures are more sensitive to the choice of solar irradiance models in the mountain location of Bolzano. If just the best-performing solar irradiance models are considered (i.e., **B20**, **C20**, **J20**), the largest annual deviations are reduced to the range from 4 to 8 kWh m^{-2} a^{-1}.

The cooling needs are characterized by larger deviations, usually occurring during the summer months (May to September) and equal to the range 6-10 kWh m^{-2} m^{-1}. June and July 2019 represent an exception, with extremely large cooling deviations, respectively equal to almost 45 kWh m^{-2} m^{-1} and almost 34 kWh m^{-2} m^{-1}. As regards the whole simulated period, the largest deviations are around 50 kWh m^{-2} a^{-1}, with the exception of the year 2019, which can reach 100 kWh m^{-2} a^{-1}. This time the largest deviation occurs with the configuration with the largest cooling energy need, i.e., the well-insulated one with a timber structure and large west-oriented windows with high *SHGC*. Analyzing the configurations with annual cooling deviations larger than 20 kWh m^{-2} a^{-1}, it can be noticed that buildings with large west-oriented windows with high *SHGC* and well-insulated envelopes are more sensitive to the choice of solar irradiance models in the considered location. If just the best-performing solar irradiance models are considered (i.e., **B20**, **C20**, **J20**), the magnitude of the largest annual deviations is reduced for 2018 and 2021, within the range from 20 to 22 kWh m^{-2} a^{-1}. On the contrary, no improvement is registered for 2019. Indeed, for this year larger *MAEs* were observed in Section 3.2 compared to the other two years, especially for north- and west-orientations, whose worst-performing pair of solar irradiance models was **J20**. Further analyses will be performed for this year in the next development of this research, studying the time series of solar irradiance values in order to identify the issues leading to these very large deviations.

The next figure shows, as an example, the cumulative distribution functions of the monthly energy needs for space heating and space cooling simulated for the 48 buildings, respectively for December 2018 and August 2018. As it can be seen, the selection of the *horizontal diffuse irradiance model* can largely affect the simulated energy needs. For instance, when model **15** (the Spencer model) is chosen, the differences among the considered *irradiance models for tilted surfaces* are more limited, for both heating and cooling needs. If model **20** (the Perez *et al.* Model 1) is picked, a larger sensitivity can be detected. As regards the heating needs, for instance, model **F** (the Ma & Iqbal model) gives different results from the rest of the group for most of building configurations. The same is true also in the case of cooling needs and a larger variability can be observed for all configurations characterized by high cooling energy demands.

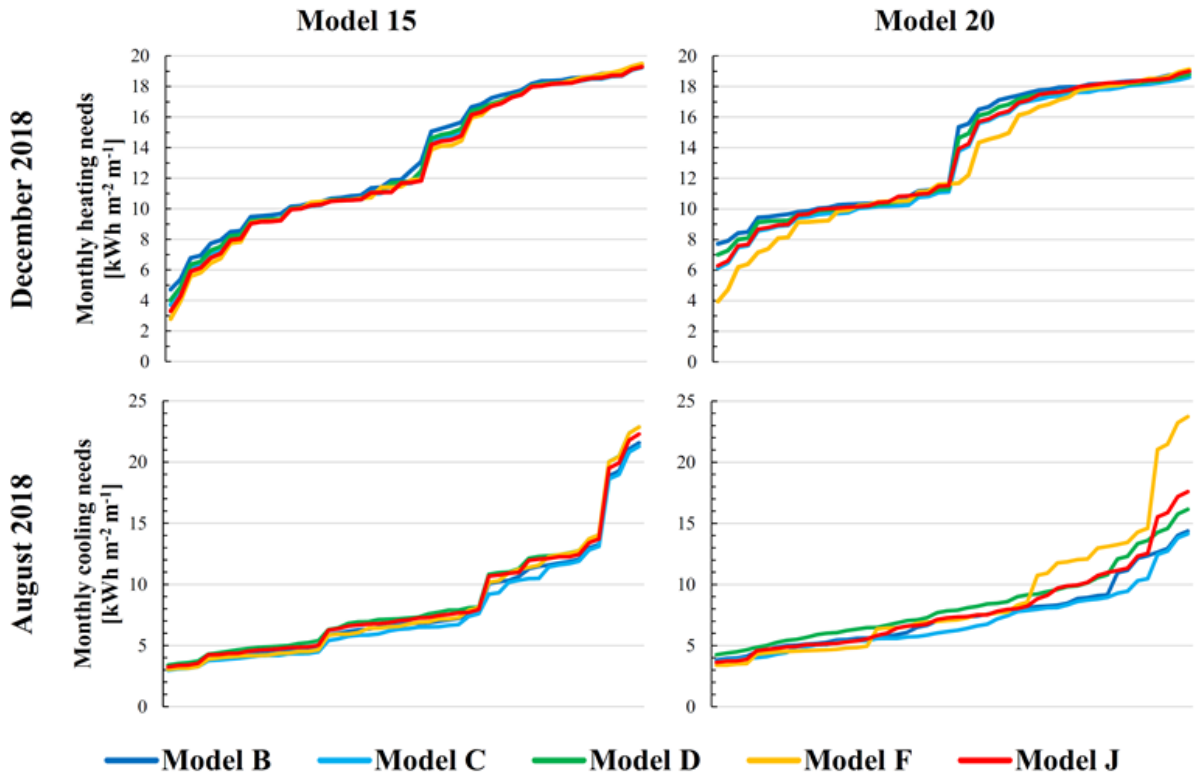

Figure 3: Cumulative distribution functions of the monthly energy needs for space heating and cooling simulated for the 48 buildings, respectively for December 2018 (top) and August 2018 (bottom). The results are distinguished according to the selected irradiance model for tilted surfaces (**B**, **C**, **D**, **F**, or **J**) and by the horizontal diffuse irradiance model (**15** on the left and **20** on the right)

4. CONCLUSIONS

In this research we analyzed the capabilities of 22 *horizontal diffuse irradiance models* and 12 *irradiance models for tilted surfaces* commonly found in the literature and in many building performance simulation codes for the calculation of the solar irradiance incident on the building envelope. The specific focus of the research was put on the simulation of solar irradiance in mountain environments, characterized by complex irradiation patterns depending on the orography and the multiple terrain reflections. In order to discuss the models' capabilities, we compared the solar irradiance calculated by all combinations of *horizontal diffuse irradiance models* and *irradiance models for tilted surfaces* with the global irradiance measured in the Alpine location of Bolzano, Italy, in the years 2018, 2019 and 2021, on four vertical surfaces oriented towards the main cardinal directions. Thanks to the analysis

of the hourly Mean Absolute Errors, the best- and the worst-performing pairs of models were identified for each year and orientations. Then, this subset of irradiance models was employed to simulate with TRNSYS 18 the energy needs for space heating and cooling for a dataset of 48 simplified buildings.
We found that:

- The performances of the pairs of irradiance models can be very different, depending on the considered orientation. The west-oriented surfaces showed the worst overall performance, probably due to the presence of natural obstacles in that direction.
- None of the models in the literature was found able to ensure the same level of accuracy for all the four vertical cardinal orientations at the same time. In some cases, a model able to minimize the errors with respect to the collected solar data in a given orientation was identified as the worst-performing one for another orientation.
- The impact of the selection of solar irradiance models on the simulated energy performance is clearly affected by the building's features. As regards the heating performance, poorly insulated buildings with massive walls and large south-oriented windows with high *SHGC* were identified as more sensitive to how the solar irradiance is modelled in the considered case-study mountain location. On the contrary, buildings with large west-oriented windows with high *SHGC* and well-insulated envelope proved to be more sensitive when it comes to the cooling performance.

Considering all the above, the next developments of this research will integrate also other weather stations and other measurements from the weather station considered in this work (e.g., beam and diffuse components of solar irradiance, besides the global values already discussed), in order to better identify the weaknesses of the existing irradiance models and suggest potential modifications to increase their capabilities first for the considered case-study location of Bolzano, Italy, and then for other Alpine environments.

REFERENCES

Boland, J., Ridley, B., & Brown, B. (2008). Models of diffuse solar radiation. *Renewable Energy*, *33*, 575–584.

Bugler, J.W. (1977). The determination of hourly insolation on an inclined plane using a diffuse irradiance modelbased on hourly measured global horizontal insolation. *Solar Energy*, *19*(5), 477–491.

Chandrasekaran, J., & Kumar, S. (1994). Hourly diffuse fraction correlation at a tropical location. *Solar Energy*,*53*(6), 505-510.

Chendo, M. A. C., & Maduekwe, A. L. (1994). Hourly global and diffuse radiation of Lagos, Nigeria - correlationwith some atmospheric parameters. *Solar Energy*, *52*(3): 247–251.

de Miguel, A., Bilbao, J., Aguiar, R., Kambezidis, H.D., & Negro, E. (2001). Diffuse solar irradiation modelevaluation in the North Mediterranean Belt area. *Solar Energy*, *70*(2), 143–153.

Dervishi, S., & Mahdavi, A. (2012). Computing diffuse fraction of global horizontal solar radiation: A modelcomparison. *Solar Energy*, *86*, 1796–1802.

Ente Nazionale Italiano di Normazione (UNI). (2014). *UNI/TS 11300-1:2014 – Energy performance of buildingsPart 1: Evaluation of energy need for space heating and cooling*, Milan, Italy: UNI.

Erbs, D. G., Klein, S. A., & Duffie, J. A. (1982). Estimation of the diffuse radiation fraction for hourly, daily andmonthly-average global radiation. *Solar Energy*, *28*(4), 293–302.

Gueymard, C.A. (1986). An anisotropic solar irradiance model for tilted surfaces and its comparison with selectedengineering algorithms. *Solar Energy*, *38*(5), 367 – 386.

Hay, J.E., & Davies, J.A. (1980). Calculation of the solar radiation incident on an inclined surface. *Proc. FirstCanadian Solar Radiation Data Workshop*, 59 – 65.

Hawlader, M.N.A. (1984). Solar diffuse, global and extraterrestrial solar radiation for Singapore. *International Journal of Ambient Energy*, *5*(1), 31 – 37.

Karatasou, S., Santamouris, M., & Geros, V. (2003). Analysis of experimental data on diffuse solar radiation inAthens, Greece, for building applications. *International Journal of Sustainable Energy*, *23*(1), 37–41.

Klucher, T. M. (1979). Evaluation of models to predict insolation on tilted surfaces. *Solar Energy*, *23*(2), 111–114.

Lam, J.C., & Li, D.H.W. (1996). Correlation between global solar radiation and its direct and diffuse components. *Building and Environment*, 31(6), 527–535.

Liu, B.Y.H., & Jordan, R.C. (1960). The interrelationship and characteristic distribution of direct, diffuse and total solar radiation. *Solar Energy*, 4(3), 1 – 19.

Ma, C.C.Y., & Iqbal, M. (1983). Statistical comparison of models for estimating solar radiation on inclined surfaces. *Solar Energy*, 31(3): 313–317.

Maxwell, E.L. (1987). A quasi-physical model for converting hourly global horizontal to direct normal insolation. *Technical Report of Solar Energy Research Institute, SERI/TR-215-3087*.

Muneer, T., Hawas, M., & Sahili, K. (1984). Correlation between hourly diffuse and global radiation for New Delhi. *Energy Conversion and Management*, 24(4), 265–267.

Muneer, T., & Younes, S. (2006). The all-sky meteorological radiation model: proposed improvements. *AppliedEnergy*, *83*(5), 436–450.

Oliveira, A., Escobedo, J.F., Machado, J.A., & Soares, J. (2002). Correlation models of diffuse solar-radiation applied to the city of São Paulo, Brazil. *Applied Energy*, *71*(1), 59–73.

Orgill, J.F., & Hollands, K.G.T. (1977). Correlation equation for hourly diffuse radiation on a horizontal surface. *Solar Energy*, 19(4), 357 – 359.

Perez, R.R., Ineichen, P., & Maxwell, E.L. (1992). Dynamic global-to-direct irradiance conversion models. *ASHRAE Transactions*, 98(1), 354-369.

Perez, R.R., Ineichen, P., & Seals, R. (1990). Modeling daylight availability and irradiance components from direct and global irradiance. *Solar Energy*, 44(5), 271–289.

Pernigotto, G., Prada, A., Baggio, P., Gasparella, A., & Mahdavi, A. (2015). Impact of solar irradiation models on simulated hourly energy performance of buildings, *BS 2015 - 14th International Conference of the International Building Performance Simulation Association*, Hyderabad, India.

Pernigotto, G., Prada, A., Baggio, P., Gasparella, A., & Mahdavi, A. (2016). Solar irradiance modelling and uncertainty on building hourly profiles of heating and cooling energy needs, *IV International High Performance Buildings Conference at Purdue*, West Lafayette, Indiana, U.S.

Pernigotto, G., Gasparella, A., & Hensen, J.L.M. (2021). Assessment of a weather-based climate classification with building energy simulation, *BS 2021 - 17th International Conference of the International Building Performance Simulation Association*, Bruges, Belgium.

Prada, A., Pernigotto, G., Gasparella, A., & Mahdavi, A. (2014a). Combined effects of diffuse fraction and tilted surface radiation models, *ECPPM 2014 - 10th European Conference on Product & Process Modelling*, Vienna, Austria.

Prada, A., Pernigotto, G., Baggio, P., Gasparella, A., & Mahdavi, A. (2014b). Effect of Solar Radiation Model on the Predicted Energy Performance of Buildings, *III International High Performance Buildings Conference at Purdue*, West Lafayette, Indiana, U.S.

Prada, A., Pernigotto, G., Cappelletti, F., & Gasparella, A. (2015). Impact of solar irradiation models on building refurbishment measures from multi-objective optimization, *BS 2015 - 14th International Conference of the International Building Performance Simulation Association*, Hyderabad, India.

Reindl, D., Beckman, A., & Duffie, J. A. (1990a). Diffuse fraction correlations. *Solar Energy*, 45(1), 1–7.

Reindl, D. Beckman, A. & Duffie, J. A. (1990b). Evaluation of hourly tilted surface radiation models. *Solar Energy*, 45(1), 9–17.

Skartveit, A., & Olseth, J.A. (1986). Modelling slope irradiance at high latitudes. Solar Energy, 36(4), 333 – 344.

Skartveit, A., & Olseth, J.A. (1987). A model for the diffuse fraction of hourly global radiation. *Solar Energy*, 38(4), 271–274.

Soares, J., Oliveira, A., Boznar, M., Mlakar, P., Escobedo, J.F., & Machado, J.A. (2004). Modeling hourly diffuse solar radiation in the city of São Paulo using a neural-network technique. *Applied Energy*, 79(2), 201–214.

Spencer, J. (1982). A comparison of methods for estimating hourly diffuse solar radiation from global solar radiation. *Solar Energy*, 29(1), 19–32.

Temps, R.C., & Coulson, K.L. (1977). Solar radiation incident upon slopes of different orientations. *Solar Energy*, 19(2), 179 – 184.

ACKNOWLEDGEMENT

This research was funded by the internal project of the Free University of Bozen-Bolzano “SOMNE - Bolzano Solar Irradiance Monitoring Network” (CUP: I56C18000930005; CRC Call 2018).